A&A 366, 913–922 (2001)
DOI: 10.1051/0004-6361:20000282

Astronomy & Astrophysics

The galactic mass injection from cool stellar winds of the 1 to 2.5 $M_\odot$ stars in the solar neighbourhood

K.-P. Schröder[1,2] and E. Sedlmayr[2]

[1] University of Sussex, Astronomy Centre, Falmer, Brighton BN1 9QJ, UK
[2] Technische Universität Berlin, Inst. f. Astronomie u. Astrophysik, Sekr. PN 8-1, Hardenbergstr. 36, 10623 Berlin, Germany

Received 20 December 1999 / Accepted 16 November 2000

Abstract. We have computed synthetic stellar samples and HR diagrams on the basis of a fine-meshed, consistent grid of evolution tracks for given IMF and SFR(t). In order to model the galactic disk stellar component (single stars only) and to derive its IMF and apparent SFR(t), we selected the synthetic sample which is the best fit to the observed distribution of single stars in the solar neighbourhood HR diagram (complete for $d < 50$ pc, $M_V \leq 4$, based on *Hipparcos* data). Most giants of this synthetic sample fall in the range of $M_\mathrm{i} = 1$ to 2.5 $M_\odot$. Stellar evolution on the tip-AGB has been computed by adopting, time-step by time-step, the mass-loss rates predicted by very detailed dust-driven, pulsating wind models for carbon-rich stars. This mass-loss description causes the natural development of superwinds. Their properties are in agreement with the range of measured masses and expansion velocities of PNe, i.e. a total mass of between 0.25 $M_\odot$ and 0.65 $M_\odot$ has been ejected over the final 30 thousand years. For the preceeding mass-loss on the AGB and RGB, we use a semi-empirical approach, i.e., a re-calibrated Reimers mass-loss which yields an RGB mass-loss (for $M_* \lesssim 1\ M_\odot$) consistent with the formation of horizontal branch stars. Combining these approaches, we obtain a consistent grid of mass-loss histories in the mass range of $M_\mathrm{i} = 1$ to 2.5 $M_\odot$. By increasing the number of stars in our synthetic solar neighbourhood stellar sample by a factor of thousand, we have been able to compute a detailed, present-day, synthetic reference sample of galactic disk RGB and AGB giant stars, together with their mass-loss. The results are in good agreement with observations of cool giant stellar mass-loss, as well as with the estimated space density of carbon stars. Finally, we discuss the relative collective yields of the RGB, AGB and tip-AGB stellar mass-loss as contributions to the galactic disk mass re-injection.

Key words. stars: evolution – stars: late-type – stars: luminosity function, mass function – stars: mass loss – Galaxy: solar neighbourhood – Galaxy: stellar structure

1. Introduction

A detailed, sophisticated model of the galactic stellar component is very much needed for any quantitative galaxy model, for example, to describe the spectral energy distribution of the integrated stellar radiation field. Furthermore, stellar ejecta play a key rôle in determining the gas/dust content of a galaxy, as well as its chemical evolution. Interstellar matter (ISM) consumed by star formation is returned by means of stellar winds and supernovae ejecta, mostly enriched by heavier elements from the nuclear processes in the stellar interior. The physics involved here, of internal mixing and stellar mass-loss mechanisms in particular, is complex and manifold, varies with stellar evolution, and is dependent on the initial stellar mass and composition.

Send offprint requests to: K.-P. Schröder,
e-mail: kps@star.cpes.susx.ac.uk

By contrast, recent galactic models (see Dwek 1998, for example) describe the stellar component with convenient but approximate scaling laws rather than making full use of the present knowledge of stellar astrophysics. But recent advances in observational techniques are now providing an ever more detailed view of the stellar component and ISM of the Galaxy, and even of very distant galaxies. Clearly, the time has come to model the galactic stellar component and its mass-loss from *first principles*: using the full knowledge of stellar astrophysics to produce representative samples of stars, based solely on the initial stellar mass function (IMF), the star formation rate (SFR), well calibrated evolutionary tracks, and a reliable, consistent mass-loss description, especially on the tip of the Asymptotic Giant Branch (tip-AGB). For this purpose, we employ the computation of synthetic HR diagrams. The comparison to HR diagrams of well-defined, complete, observed samples of stars provides a very

powerful tool for the derivation of a realistic, detailed model of the galactic stellar component.

While the mass circulation of young galaxies is dominated by the short-lived, very massive stars which end as super-novae, the situation is significantly different for a settled galactic environment such as the solar neighbourhood. Here, many of the numerous low-mass stars, down to about 1 $M_\odot$, have had time to evolve into the Red Giant Branch (RGB) or the AGB, where they contribute to the collective cool wind stellar mass-loss. In fact, we show (Sects. 4 and 5) that the stars with initial masses in the range of 1 to 2.5 $M_\odot$ make a significant contribution to the galactic mass re-injection. This is because (a) all less massive stars evolve too slowly to have yet arrived on the RGB, which marks the onset of cool winds. (b) In the higher mass regime, the steeply decreasing IMF severely reduces stellar numbers. Present-day stellar numbers are decreasing even more strongly with increasing mass because of their much faster evolution.

In this work, attention is focused on the evolution and mass-loss of low-mass stars in the range of 1 $M_\odot$ to 2.5 $M_\odot$. Our self-consistent, hydrodynamic dust-driven wind models (see Fleischer et al. 1992; Arndt et al. 1997, and references therein) describe in detail the mass-loss of a carbon-rich tip-AGB star of given present-day mass (0.8 to 2 $M_\odot$), luminosity, and effective temperature. In combination with evolutionary models, we have been able to follow such giants, time-step by time-step, into their superwind phase (Schröder et al. 1999). Here and in the following text, "tip-AGB" refers to the short, but crucial final phase of AGB evolution, while "AGB" refers to the majority of AGB stars which are still ascending comparatively slowly, with moderate mass-loss.

Our computations yield complete mass-loss histories which show that a large fraction of the total stellar mass-loss is indeed achieved on the tip-AGB, after the stellar atmosphere has turned carbon-rich. These mass-loss histories are very consistent with the formation of planetary nebulae (PN), and they include a first quantitative model for the remarkably thin CO shells of a few carbon stars as found by Olofsson et al. (1996, 2000).

We use a fine-meshed grid of evolutionary tracks and corresponding mass-loss histories to obtain a detailed model of the collective cool wind stellar mass-loss of the solar neighbourhood stellar population, by means of a synthetic present-day giant star sample, and by computing the sample-integrated mass-loss yields. The procedure can be broken down into the following sequence of steps:

1. Computation of a grid of evolutionary tracks, including a consistent and thorough treatment of mass-loss;
2. Computation of a synthetic stellar sample and HR diagram by randomly distributing stars on the grid of evolutionary tracks. With the average initial mass-distribution given by the IMF, and the average age distribution given by the SFR(t), the resultant sample should match a well defined, complete observed sample (i.e., the solar neighbourhood as a representative sample of galactic disk stars);
3. Creation of an inventory of this sample: which stars really contribute to the collective present-day mass loss?
4. Computation of a much enlarged sample of stars as a sufficient basis for a present-day reference-sample of giants and their mass-loss, including enough stars to represent the brief tip-AGB phase;
5. Integration of stellar mass-loss over the RGB, AGB and "superwind" life-times, and over the stellar sample, to obtain the specific collective yields for the galactic gas and dust (re-)injection rates.

2. Evolution models and mass-loss description

Here we have used the well tested evolution code of Peter Eggleton (see Eggleton 1971, 1972, 1973; Pols et al. 1998). Metallicity ($Z = 0.02$) and overshoot prescription were the same as used with the best-performing grid of evolutionary tracks (No. 4) by Schröder (1998), i.e., no overshooting for $M_\mathrm{i} < 1.75\ M_\odot$, $\delta_\mathrm{ov} = 0.06$ at 1.8 $M_\odot$, and $\delta_\mathrm{ov} = 0.12$ for $M_\mathrm{i} > 1.85\ M_\odot$. The latter value corresponds to overshoot lengths l_ov which increase slightly with stellar mass, i.e., from 0.22 pressure scale heights for 2 $M_\odot$ to 0.32 for 6.5 $M_\odot$. In this mass range, the overshooting parameter was calibrated by modelling the physical properties of ζ Aur systems (Schröder et al. 1997).

A consistent mass-loss description was used to rederive the actual stellar mass after each time-step, for each evolution track (see Schröder et al. 1999). This is of particular importance when approaching the tip-AGB, where the mass-loss varies significantly (see Fig. 1), and where its influence on stellar evolution at large creates a complex feed-back. We derived our tip-AGB mass-loss rates from the detailed, dust-driven and pulsating wind models of Fleischer et al. (1992) for carbon-rich stars. The complex physics involved in such dust-driven winds has been reviewed by Sedlmayr (1994) and Sedlmayr & Winters (1997).

The dust-driven wind models from Fleischer et al. (1992) are highly sensitive to stellar effective temperature, and depend on a minimum luminosity, which is required to drive such a wind (and which varies with M_* and T_eff). Another input parameter is the C:O surface abundance ratio, which the evolution code is presently unable to solve. But because the mass-loss rate does not depend very critically on the exact C:O ratio, an appropriate value may actually be derived on the basis of reasonable assumptions. This has previously been discussed by Schröder et al. (1999), where the influence of the wind characteristics on tip-AGB evolution and the related mass-loss were studied in detail, especially for the "superwind" phase (Renzini 1981) during the final 30 000 yrs. Figure 1 gives a representative example of the tip-AGB mass-loss evolution in our models.

For the mass-loss history prior to the onset of carbon-rich winds, we use an empirical description, mainly given by the Reimers formula (1975), where $\dot{M} = \eta \cdot 4\ 10^{-13} \cdot LR/M$, with all stellar quantities measured in solar units,

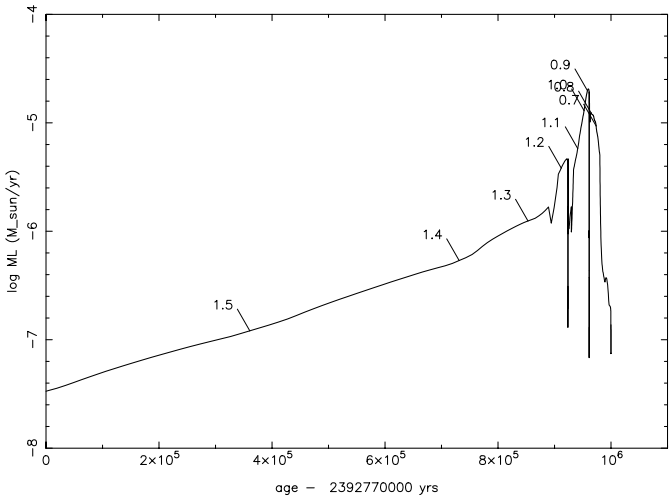

Fig. 1. The final million years of a (typical) tip-AGB mass-loss, as obtained with the $M_\mathrm{i} = 1.6\ M_\odot$ model listed in Table 2. Note the accelerated reduction of the actual stellar mass (given in $M_\odot$ as indicated), towards the tip-AGB

and time in years. With our evolution models, $\eta = 0.2$ is required to obtain mass-loss yields from low-mass RGB stars which are consistent with the subsequent formation of horizontal branch stars. Further up on the AGB, just before the onset of carbon-rich winds, mass-loss is described by the empirical formula of De Jager et al. (1988), with ramps for the transistions (see Schröder et al. 1999).

Our complete grid of evolution tracks covers the large range of $M_\mathrm{i} = 0.7$ to 16 $M_\odot$, in order to adequately represent high stellar masses in the synthetic stellar samples. A maximum track density of $\Delta\, M_\mathrm{i} = 0.05\ M_\odot$ was chosen for the much more highly populated lower mass range. Up to $M_\mathrm{i} = 2.5\ M_\odot$, all evolution models were pursued to the very tip of the AGB, fully covering the superwind phase found with these stars, and allowing a study of the complete mass-loss. Computations for larger stellar masses, however, became too CPU-intensive near the tip-AGB to carry out, and their mass-loss histories remain incomplete. The computed mass-loss for the models between 0.95 and 2.5 $M_\odot$ is discussed in more detail in Sects. 4 and 5, where a list of the individual evolution models is given in Table 2.

Our upper mass-limit M_up for stars reaching the AGB is 6.1 $M_\odot$ (see Pols et al. 1998). The initial–final Mass (M_i, M_f) relation obtained in the range of $M_\mathrm{i} = 1.0$ to 2.5 $M_\odot$, can be approximated by $M_\mathrm{f}/M_\odot = 0.55 \cdot (M_\mathrm{i}/M_\odot)^{0.29}$. This is in reasonable agreement with recent studies in this field. In particular, our 2.5 $M_\odot$ model gives only a slightly larger (0.04 $M_\odot$) mass than the respective empirical value of $M_\mathrm{f} = 0.68\ M_\odot$ derived by Weidemann (1997) from the Hyades stellar cluster. Otherwise, our final masses are in excess of the relation suggested by Iben et al. (1996) and Weidemann (1997) by 0.02 $M_\odot$ (M_i around 1.5 $M_\odot$) to 0.05 $M_\odot$ (M_i around 2.5 $M_\odot$), and that of Herwig (1996) by less than 0.07 $M_\odot$. The latter work represents the lower range of suggested M_f values.

3. Re-visiting the local IMF and apparent SFR(t)

In the past, IMF and SFR have already been studied in detail (see Miller & Scalo 1979; Scalo 1986). The stellar luminosity function of galactic field stars was derived from a large statistical sample, but inherent uncertainties remained from inaccurate absolute luminosities, and from a more approximate transformation of the luminosity function into a mass function.

For galactic field stars more massive than the Sun, Scalo (1986) obtained an IMF of $\frac{\mathrm{d}\,N_*(M_*)}{\mathrm{d}\,\log_{10}(M_*)} \propto M_*^\gamma$, with a slightly mass-dependent, average γ-value of about -1.7.

Meanwhile, *Hipparcos* parallaxes have provided significantly more accurate absolute luminosities. Also, stellar evolution models are now very well constrained and thoroughly tested, and can much more reliably link the stellar mass function to the observed luminosity function. We have shown (Schröder 1998) that synthetic HR diagrams are a very useful tool when matching an observed, *complete* sample of stars: Stellar number counts along the main sequence (MS) are *directly* related to the present-day mass-function (PDMF), which therefore can be derived from *first principles*. In particular, the mass-dependent fraction of post-MS stars missing in the MS star counts is consistently been accounted for by the synthetic HR diagram.

Our earlier work, however, relied on one critical approximation: that SFR and IMF remains unchanged over a period of time *longer* than the life-times $\tau(M_*)$ of the stars in question. In this case (approach a), the rate of stars finally leaving the AGB by becoming white dwarfs (WDs) becomes equal to the time-independent rate of star formation: $\mathrm{PDMF}/\tau(M_*) = \mathrm{IMF} \times \mathrm{SFR}$, and the PDMF is time-independent, too. This approach is restricted to stars which have life times comfortably shorter than the age of their galaxy.

With a time-independent PDMF, synthetic HR diagrams may be computed with two simplifications: (i) Considering the *present-day* stars only (excluding WDs) and using the PDMF to arrange their mass distribution, and (ii) by using relative time scales normalised by the respective life times. This projects the random age distribution of all present-day stars simply into the same interval, i.e., between 0 and 1, and greatly simplifies the interpolation process required for placing the stars on the evolution track grid.

The assumption of a constant SFR, however, appears to break down for stars less massive than 1.6 $M_\odot$ (Schröder 1998). In order to derive the IMF more accurately, and to compute synthetic HR diagrams which include reliable numbers of less massive and older stars, we need to take full account of a possibly different apparent SFR(t) of the old stars. By "apparent SFR", we mean the difference between the genuine SFR(t), looking back in time, and the fraction of stars (age t) lost from the solar neighbourhood through diffusion. Any such net-loss (more stars leave the galactic disk than are gained from the halo) has the same effect as if those stars were never formed.

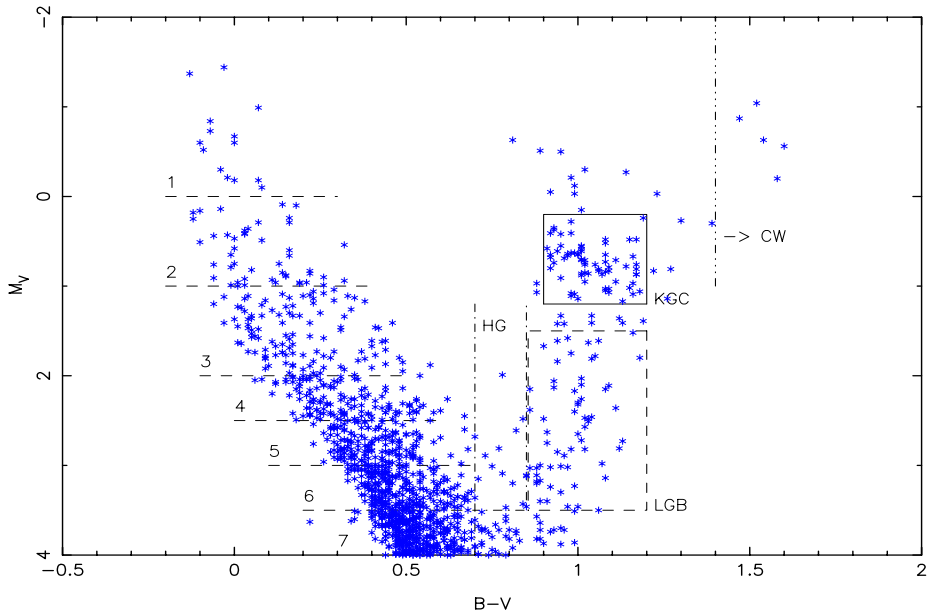

Fig. 2. HR diagram of the solar neighbourhood for $d < 50$ pc, as observed by Hipparcos (single stars only). Indicated regions and their star counts are listed in Table 1 for a comparison with synthetic HR diagram. Regions 1 (no upper boundary) to 7 contain main sequence stars of different masses, HG represents the Hertzsprung gap, LGB the lower (Red) Giant Brach, KGC the "K giant clump", and CW the stars with cool winds

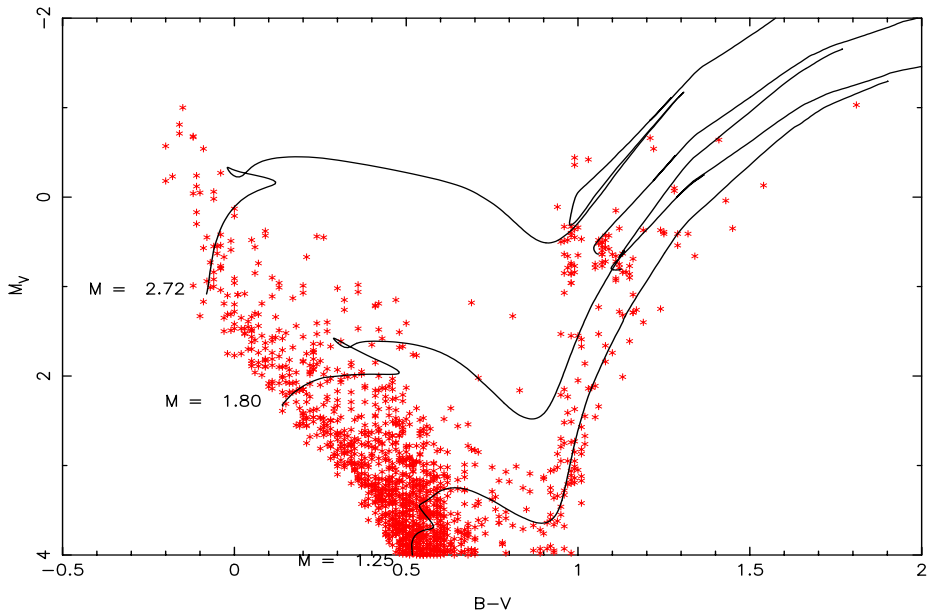

Fig. 3. Synthetic HR diagram, computed to match Fig. 2, using an IMF with $\gamma = -1.7/-1.9$ for $M_* < / > 1.8\ M_\odot$, respectively, and an apparent (see text) SFR(t) of 1 14 $10^{-6} \cdot \mathrm{e}^{-t/6.3\ \mathrm{Gyr}}$ $*$ /yr (stars within 50 pc and exceeding 0.9 $M_\odot$)

Consequently, the genuine SFR and any accumulated net-losses from a limited volume remain inseparable, and the apparent SFR may well decrease when looking backwards in time. With such a variable apparent SFR(t), the PDMF varies with time, even though we may still assume a time-independent IMF.

To solve this problem here, we use the *direct* approach for forming a synthetic stellar sample (approach b). Hence, we must consider *all* stars formed in the past, with a random choice of mass and age, but under the condition that the given IMF and SFR(t) are obeyed. Here, of course, stellar ages are ascribed on the absolute time-scale. All stars are then checked, whether they are still on their evolution track, or whether they have already passed the AGB.

Although approach (b) appears to be straight forward, it is a demanding task for the interpolation procedure: Stellar life times vary strongly with mass, and placing the stars correctly in a grid of evolution tracks on an absolute timescale requires a much finer spacing of the models in

stellar mass. Mostly, we found that $\Delta M = 0.05\ M_\odot$ is adequate, which requires about three times as many evolution tracks than needed for approach (a). In addition, with the recent inclusion of realistic and consistent stellar mass-loss in our evolution models (see Sect. 2) we have significantly improved the representation of giant stars and of tip-AGB stars in particular.

As an observed reference stellar sample, we used the same complete selection of single solar neighbourhood stars ($d < 50\,\mathrm{pc}$) from the *Hipparcos*-catalogue as described by Schröder (1998). This sample is representative of the average galactic disk stellar component, binaries excluded, of the Galaxy: the solar neighbourhood is sufficiently mixed and is not biased by its location with respect to spiral arms and the galactic centre. We restricted the *Hipparcos*-sample to the fairly small maximum distance of 50 pc from the sun in order to maintain completeness for $M_v < 4$. After the exclusion of all known binary stars, this sample contains a reasonable number of 1340 single stars (Fig. 2).

In order to find the best match with the observed HR diagram, we computed a number of synthetic HR diagrams for different combinations of IMF and SFR(t). For each, number counts of stars in characteristic regions in the HR diagram (indicated in Fig. 3) were compared to the respective counts of observed stars.

The IMF was determined by comparing the population density along the MS (regions 1 to 7), which requires adjustment of the resulting PDMF. The MS star counts are particularly sensitive to the IMF, because stellar mass and MS luminosity are related in a well-defined way, for any given metallicity. However, as the mean stellar age on the MS increases towards lower luminosity, any matching, preliminary IMF for lower mass stars depends partly on how the SFR(t) was chosen. An obviously artificial, strong change of γ in the IMF around $M_\mathrm{i} = 1.6\ M_\odot$ was found by Schröder (1998) when using a constant SFR. We here introduced an exponential decline of the SFR(t) with stellar age t and started with a preliminary timescale τ_0 of 6 Gyr to derive a preliminary IMF. This largely removes the artificially strong change of γ.

For any current, preliminary IMF we verified the initial choice of SFR(t), i.e., of its time scale of change τ_0. We based this procedure on matching the number counts of those post-MS regions in the HRD which best represent different age groups. The very oldest stars (about 10^{10} yrs) are clearly found in the lower RGB (region "LGB"). They have a mass of around 1 $M_\odot$, still well clear of our mass cut-off at 0.9 $M_\odot$, and advance only very slowly on the RGB. By comparison, the K giant clump (region "KGC") contains the He-burning stars with about 1.2 $M_\odot$ to 2 $M_\odot$ and represents giants of intermediate age. Furthermore, both these regions are comparably well populated. Consequently, the LGB/KGC number ratio became our criterion to optimise of τ_0. Changing τ_0 also changes the population density in the lower MS regions, but not so strongly. Slight adjustments of the γ-value for the IMF are therefore required with each attempt to find a better-matching SFR.

The finally best fitting synthetic HR diagram is shown in Fig. 3, and its number counts are listed in Col. S of Table 1. The respective synthetic stellar sample was computed with an IMF of $\gamma = -1.9$ for $M_* > 1.8\ M_\odot$, and $\gamma = -1.7$ for any lower masses, and with a SFR(t) of $1.14\ 10^{-6} \cdot \mathrm{e}^{-t/6.3\ \mathrm{Gyr}} * /\mathrm{yr}$ for single stars within 50 pc, which exceed 0.9 $M_\odot$. Here, t gives the age of the stars formed, and SFR(0) is the present star formation rate, equivalent to $2.2\ 10^{-3}$ stars formed per kpc^3 and year. Together, this consumes a total mass of $4.5\ 10^{-3}\ M_\odot$/yr in a volume of one kpc^3.

The majority of the synthetic stars created are MS stars not far from the low-mass cutoff, which miss the minimum brightness of $M_v = 4$. Therefore, only a fraction of each synthetic sample actually compares with the observed sample, and the number of sufficiently bright stars cannot be precisely set since it shows some statistical fluctuation. These low mass stars need to be considered, however, since a large proportion of present-day giants have evolved from them.

The number counts obtained from our best-matching synthetic HR diagram agree very well with those from the observed HR diagram (Col. O in Table 1), with the single exception of a predicted deficiency of stars in the MS region No. 4. This discrepancy could hint a period of a reduced local SFR around 1.2 Gyr ago, or a short-lived SFR peak roughly 1.9 Gyr ago. The latter is close to the age of the Hyades, and we have modelled this scenario; Col. S' of Table 1 gives the resulting star counts. By comparison to sample S, a total of 10^3 stars formed 1.9 Gyr ago were added to a slightly reduced SFR (by 13%) with a somewhat smaller exponent γ (by 0.1). Considering all star counts together, however, no significantly better match is achieved with sample S'. We therefore adopted the simpler specifications of sample S. Most differences to the observed sample O do not exceed the square root of the respective number count, which is the statistical variation.

We find that the net diffusion losses of older stars in the solar neighbourhood from the galactic disk into the halo outnumber any possible effect of a genuinely larger past SFR, because we need to adopt an apparent SFR which decreases exponentially towards the past. The oldest stars, giants of about 1 to 1.2 $M_\odot$ which populate the lower RGB (region LGB in Fig. 2), are significantly reduced in number in comparison with synthetic HR diagrams based on no or smaller diffusion losses. An increase of the apparent SFR timescale from 6.3 to only 7.2 Gyrs, along with the required γ adjustment of the IMF (-1.5 instead of -1.7 for $M_\mathrm{i} < 1.8\ M_\odot$, which maintains the observed population density on the MS), already results in a statistically significant increase of the count ratio LGB/KGC by around 20%. For changes of only 0.1 in γ, however, there remains ambiguity between slightly different combinations of IMF(M_i) and SFR(t), especially in the range of low-mass and old stars.

Table 1. Comparison of the number counts in characteristic HR diagram regions between the observed (O, see Fig. 2) and the best matching synthetic stellar samples S (see Fig. 3) and S' (see text for details)

Region	Samples:	O	S	S'
1		15	15	15
2		47	45	43
3		114	124	116
4		134	98	112
5		174	175	188
6		266	275	296
7		384	393	402
KGC		70	64	66
HG		16	14	16
LGB		64	73	73
CW		5	7	6
total		1338	1380	1380

4. A synthetic present-day sample of galactic disk giants and their mass-loss

Stars which undergo reasonable mass-loss are all comparatively short-lived, as can be seen from the low count of the cool wind (CW) region in Fig. 2. To compute a large enough, representative sample of giants, we enlarged the stellar numbers of sample S by a factor of 1000. Figure 4 shows the resulting distribution of initial stellar masses of, specifically, the synthetic RGB and AGB giants, which we restricted to colours of $(B-V) \geq 1.40$. The mass-range of 1.0 to 2.5 $M_{\odot}$, on which we are focusing this paper, clearly contains the large majority of present-day giants.

Figure 5 shows a plot of the synthetic, present-day distribution of mass-loss rates of these same RGB and AGB giants. Rates of a few 10^{-9} $M_{\odot}$/yr by far the are most frequent. They occur with the many lower mass and less evolved giants, which evolve slower than more massive giants and stars further up on the AGB. There is also a tail of strong mass-loss ("superwinds"), up to several 10^{-5} $M_{\odot}$/yr, of stars at the very tip-AGB. These few but massive winds are about equally important for the galactic mass re-injection than the many giants with much smaller mass-loss (see the following section). For this reason, we show the specific tip-AGB, initial-mass distribution and the tip-AGB, mass-loss rate distribution in two extra plots (Figs. 6 and 7) selecting only the giants with $T_{\rm eff} < 2700$ K.

A direct comparison of the theoretical mass-loss distribution with observations is presently not possible, for two reasons: (i) Mass-loss rates are difficult to derive from observations (see Habing 1994). In addition, they depend on exact distances which are still unavailable for most objetcs. (ii) Observed samples of galactic objects are not complete and not volume-limited. At best, they are flux-limited (Groenewegen et al. 1992) or selected by a mass-loss indicator (Whitelock et al. 1994). The recent ISOGAL survey (Glass et al. 1999) resulted in a very rich, flux-limited sample of red giants in the galactic bulge (Omont et al. 1999), but the data still await interpretation in terms of mass-loss rates. In addition, the SFR history of the galactic bulge seems to differ from that of the solar neighbourhood, on which we have modelled our synthetic samples. We should also mention the new flux-limited samples of Magellanic Cloud giants (Cioni et al. 2000), based on DENIS data, which are in fact complete and volume-limited. But our current models do not account for the required non-solar metallicities.

Still, a qualitative comparison of the range of observed mass-loss rates, in particular of its upper end at about $10^{-4.7}$ $M_{\odot}$/yr (Whitelock et al. 1994), yields good agreement with the rate distribution of our synthetic sample. The same authors also note that mass-loss rates of stars with the same period typically differ by an order of magnitude, while Josselin et al. (2000) find no clear correlation between mass-loss and luminosity. Our synthetic stellar sample fully confirms these observations: stars of different

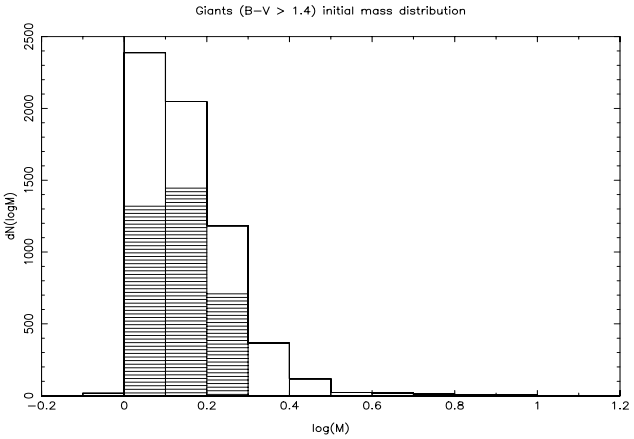

Fig. 4. Distribution of initial masses of a synthetic present-day sample of giants, based on the same IMF and SFR as for Fig. 3, but for a stellar sample enlarged by a factor of 1000. Shown are counts dN in mass intervals of $\Delta\log(M_*) = 0.1$, for RGB (hatched) and AGB stars

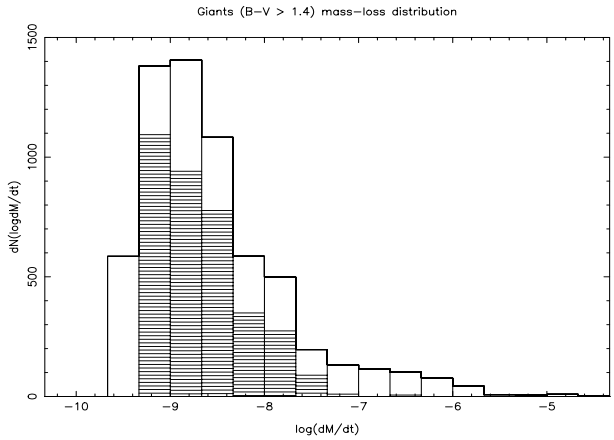

Fig. 5. Mass-loss rate distribution of the same synthetic present-day giant star sample as in Fig. 4. Shown are counts dN in mass-loss intervals of $\Delta\log(\dot{M}) = 1/3$, for RGB (hatched) and AGB stars

mass enter the superwind phase at somewhat different luminosities. Consequently, AGB stars of the same luminosity show a range of mass-loss rates.

Furthermore, Groenewegen et al. (1992) describe an observed sample of galactic carbon stars, from which they derive a total space density of 185 carbon stars per kpc^3. Our 1000× enlarged solar neighbourhood sample ($d <$ 50 pc) has 139 giants with $T_{\rm eff} < 2700$ K (those shown in Figs. 6 and 7), including both carbon-rich *and* oxygen-rich stars. This corresponds to a total space density of 265 tip-AGB giants per kpc^3, which is in good agreement with the above number for the carbon stars alone. Also, the mass-loss rates derived from the above carbon star observations range from many stars with mass-loss just over 10^{-7} to a few cases in excess of $10^{-5} M_\odot$/yr, in good agreement with our synthetic tip-AGB mass-loss distribution (Fig. 7).

Since our evolution code presently does not yield the exact C:O surface abundance ratio, we are unable to identify the carbon stars in our synthetic sample. We can, however, estimate how many there should be: recent evolution models suggest that carbon stars evolve from a lowest initial mass of 1.5 $M_\odot$, while hot-bottom burning limits the formation of carbon stars with intial masses larger than about 4 $M_\odot$ (see Groenewegen et al. 1995, and references therein). Of our synthetic tip-AGB stars in Fig. 6, about 60% or nearly 160 */kpc^3 (versus 185 */kpc^3 derived by Groenewegen et al. 1992) are found in that mass range. Hence, we believe that our synthetic sample of giants and tip-AGB stars is a reliable model and good theoretical reference sample of the respective stars found in the solar neigbourhood.

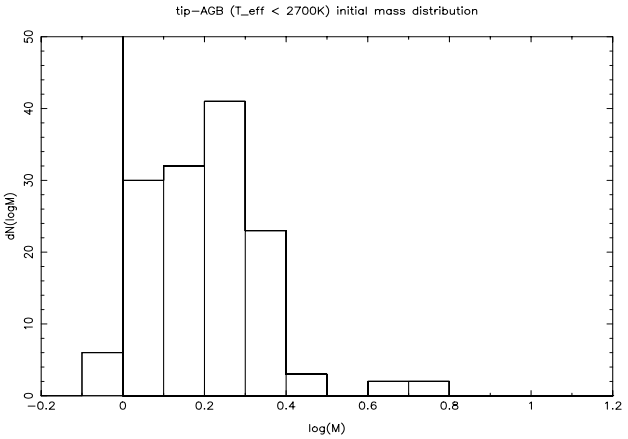

Fig. 6. Distribution of initial masses, on a logarithmic scale, of the same 139 tip-AGB giants shown in Fig. 4

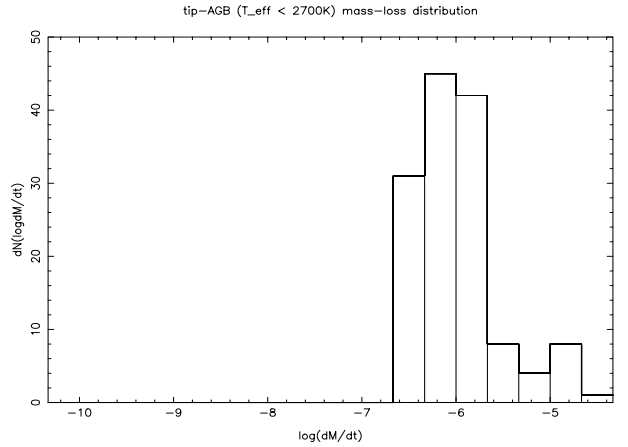

Fig. 7. Mass-loss rate distribution of the subsample of the 139 tip-AGB giants ($T_{\rm eff} < 2700$ K) from the synthetic sample shown in Fig. 5

5. Mass-loss yields from cool winds of RGB and AGB stars

So far, we have discussed the mass-loss rates of individual, present-day giants. From a galactic point of view, however, stellar mass-loss matters in terms of its life-time-integrated yields, which are visualised in Fig. 8 for the range of $M_{\rm i} = 0.95$ to 2.5 $M_\odot$. For this mass range, we like to distinguish between the mass-loss yields achieved during the more long-lived phases of ascending the RGB and the AGB ($\Delta M_{\rm AGB}$ and $\Delta M_{\rm RGB}$ in Table 2), both associated with moderate mass-loss rates, and the superwind-related, carbon-rich yields of the final 30 000 years on the tip-AGB ($\Delta M_{\rm tAGB}$). Note, that (i) the mass lost on the RGB is only significant for low mass stars, and (ii) that among the stars with larger initial mass, $\Delta M_{\rm AGB}$ increases more steeply with mass than $\Delta M_{\rm tAGB}$.

From the individual mass-loss yields we now want to derive the collective mass-loss yields for a whole stellar sample. In Sect. 4, we have shown that the stars in the mass range of 1.0 to 2.5 $M_\odot$ account for the overwhelming *number* of giants in a present-day sample. But because of the very different life-times of the different kind of giants, very short-lived but massive giants have a larger impact on collective yields than it may seem from their low numbers in a the present-day sample of giants. We therefore begin with investigating how representative the above mass range is for the total *mass* of the galactic stellar component.

For the sake of simplicity, we here introduce two approximations: (i) We use a simpler IMF with a constant $\gamma = -1.8$, which is only marginally different from the IMF derived in Sects. 3 and 4, and which on a linear mass scale is equivalent to $\frac{{\rm d}\,N_*(M_{\rm i})}{{\rm d}\,M_{\rm i}} \propto M_{\rm i}^{-2.8}$. (ii) We consider the simple case of a constant SFR, since any changes of the apparent SFR(t) found in Sect. 3 are only on a long timescale of more than 6 billion years, dominated by the diffusion of stars into the galactic halo rather than any genuine changes of the SRF.

Assuming a constant SFR, equality is reached for each $M_{\rm i}$ between the time-independent rates of stars presently been formed (IMF($M_{\rm i}$) × SFR), of stars presently dropping out of any mass-loss when ending as a WD, and of stars entering, for example, their superwind phase. The present mass-consumption rate of the stellar sample, as well as its present total mass-loss rate in a given $M_{\rm i}$ range then simply scales with the IMF($M_{\rm i}$). In terms of total

Table 2. An account of the initial stellar masses, masses lost on the RGB, masses lost on the AGB (excluding the superwind), masses lost by the superwind (i.e., in the final 30 000 years before the collapse of the superwind), and the computed final stellar masses, all in units of $M_\odot$. The bottom line gives the relative yields of the collective mass-loss of a solar neighbourhood stellar sample (see Sect. 5) in this mass range

$M_{*,\mathrm{i}}$	ΔM_{RGB}	ΔM_{AGB}	ΔM_{tAGB}	$M_{*,\mathrm{f}}$	
0.95	0.37	0.04	—	0.54	
1.00	0.24	0.20	—	0.55	
1.05	0.16	0.30	—	0.56	
1.10	0.12	0.38	0.01	0.56	[1])
1.15	0.11	0.41	0.04	0.57	[1])
1.20	0.09	0.40	0.09	0.58	[1])
1.25	0.08	0.32	0.23	0.59	[1])
1.30	0.08	0.34	0.26	0.60	
1.35	0.07	0.34	0.28	0.60	
1.40	0.07	0.41	0.28	0.61	
1.45	0.06	0.45	0.28	0.61	
1.50	0.06	0.48	0.31	0.62	
1.55	0.06	0.49	0.35	0.62	
1.60	0.05	0.52	0.38	0.63	
1.65	0.05	0.52	0.41	0.63	
1.70	0.05	0.58	0.39	0.64	
1.75	0.04	0.60	0.44	0.64	
1.80	0.03	0.69	0.44	0.65	[2])
1.85	0.02	0.69	0.48	0.65	
1.90	0.015	0.72	0.49	0.66	
1.95	0.01	0.75	0.50	0.66	[3])
2.05	0.005	0.84	0.51	0.67	
2.15	—	0.89	0.54	0.68	
2.25	—	0.95	0.55	0.69	
2.35	—	1.00	0.60	0.70	
2.50	—	1.10	0.65	0.72	
Sample:	f_{RGB}	f_{AGB}	f_{tAGB}	$f_{\mathrm{M-fin}}$	
	0.065	0.334	0.167	0.434	[4])

[1]) Only brief superwind burst(s).
[2]) Onset of core overshooting on MS at $M_{*,\mathrm{i}} \approx 1.8\ M_\odot$.
[3]) RGB evolution ends with He flash for $M_{*,\mathrm{i}} \leq 1.95\ M_\odot$.
[4]) Fraction of stellar mass returned by a sample (1.0 to 2.5 $M_\odot$, IMF $\propto M_*^{-1.8}$) – see Sect. 5.

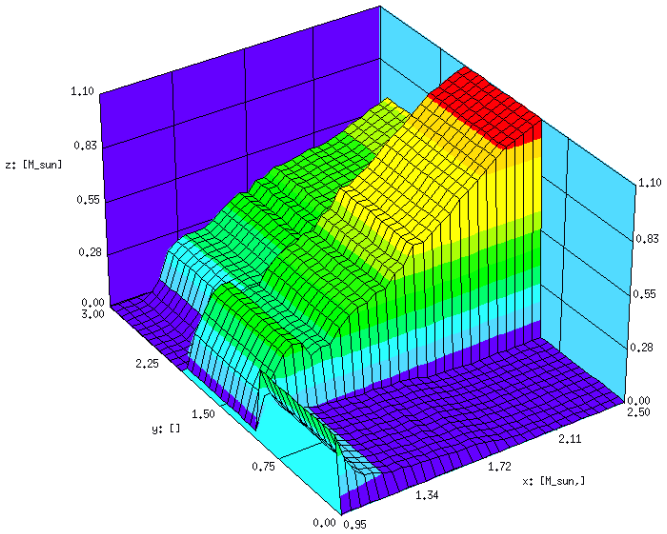

Fig. 8. Graphical comparison of the stellar mass-loss yields on the RGB (in front), the AGB (middle), and the tip-AGB "superwinds" (in the back), as listed in Table 2. Total mass lost is shown (z-axis) as a function of initial stellar mass (x-axis)

mass, a simple integration over IMF $\times M_\mathrm{i}$ shows that the formation of stars between 1.0 and 2.5 $M_\odot$ accounts for almost *half* (48%) of the mass of *all* stars formed with more than 0.9 $M_\odot$ and being relevant for the galactic mass re-injection of a sufficiently old galaxy. Even without any knowledge of the mass-loss from the stars with $M_\mathrm{i} > 2.5\ M_\odot$, we may therefore state that any significant fraction of mass redistributed by the cool winds of stars with $M_\mathrm{i} < 2.5\ M_\odot$ is still a significant fraction of the mass-loss of the whole stellar component.

Altogether, stars in the mass-range of 1.0 to 2.5 $M_\odot$ consume interstellar matter at a present rate of about 2.2 10^{-3} $M_\odot$/yr in a volume of one kpc^3. If the SFR is constant, collective yields of lost mass can conveniently be expressed as fractions of the above rate. Estimates of these fractions are listed in the bottom line of Table 2, as obtained by integration over the individual mass-loss yields, weighed with an IMF with $\gamma = -1.8$:

$$f_{\mathrm{AGB}} = \int_1^{2.5} \Delta M_{\mathrm{AGB}} \cdot M_\mathrm{i}^{-2.8} \mathrm{d}M_\mathrm{i} \Big/ \int_1^{2.5} M_\mathrm{i}^{-2.8} \mathrm{d}M_\mathrm{i}$$

(e.g.).

We here like to note that the assumption of a constant SFR and the resulting steady state of the stellar sample yields the same fractions of collectively lost mass as a stellar sample which was created in a single, short star burst. Of course, this approximation of a steady state holds only for those stars short-lived enough to have completed their whole course of stellar evolution in a time shorter than at least the age of the Galaxy. Near our low-mass cut-off ($M_\mathrm{i} \lesssim 1\ M_\odot$), all respective stars are still on the MS and do not contribute to the present-day mass-loss.

Figure 8 shows how the individual mass-loss yields ΔM_{AGB} and ΔM_{tAGB} increase with M_i. For the relative contributions to the collective yields, both functions have to be multiplied with the IMF which is strongly decreasing with M_i. The resulting differential, collective yields, from intervals in M_i, all decrease towards larger M_i, as shown by Fig. 9. While the RGB mass-loss yield is extremely biased towards the low mass end, we can see that the tAGB and AGB contributions are much more evenly covering mass space. However, both clearly reach their maxima below $M_\mathrm{i} = 1.4\ M_\odot$ and then decrease steadily with M_i.

Hence, we may indeed claim that the mass range of 1 to 2.5 $M_\odot$ is very important for the return of stellar mass into the ISM, at least for a sufficiently evolved stellar population as found in the solar neighbourhood.

For the total collective stellar mass re-injection, finally, we would like to emphasize the following aspects of our results:

1. A large fraction of the mass consumed by stars between 1 to 2.5 $M_\odot$ remains forever gravitationally trapped in the stellar remnants ($f_{\mathrm{M-fin}} = 0.43$). But altogether, 57% of the stellar mass is "re-cycled", mostly been enriched with processed material;
2. Stars below about 1.1 $M_\odot$ lose a significant amount of their mass already on the RGB (as shown in Fig. 8). The reasons are that they become cool and luminous objects on the RGB, and by comparison to more massive stars spend much more time in that phase. Hence, the RGB mass-loss yield of low mass RGB stars accumulates, while it is insignificant with larger stellar mass. On the AGB, low mass stars then fail to start a carbon-rich "superwind". Consequently, their contribution to the galactic mass-injection (almost all of f_{RGB}) is mainly *oxygen-rich*, though partly enriched by processed matter (Wasserburg et al. 1995);
3. Pre-"superwind" AGB mass-loss (f_{AGB}) returns 1/3 of all mass consumed by stars between 1 and 2.5 $M_\odot$;
4. Carbon-rich "superwinds" at the tip-AGB should occur with stars more massive than 1.3 $M_\odot$, assuming that the dredge-up of carbon-rich material by thermal pulses works for such giants. The collective return of stellar mass by "superwinds" (f_{tAGB}) then returns about 1/6 of all mass consumed by the solar neighbourhood stars between 1 and 2.5 $M_\odot$. To the total yield of re-injected carbon-rich gas, this is only a lower limit, because some pre-superwind mass-loss of carbon stars from below the critical superwind luminosity has to be included here;
5. No mean dust-to-gas ratio of the mass re-injected into the galactic ISM by stellar winds can presently been given, and we can make only a rough estimate for the carbon-rich wind ejecta: Our respective wind models show that the dust yield depends quite critically on the exact C:O abundance ratio for the tip-AGB carbon-rich ejecta. According to our wind models with C:O = 1.3, a representative dust-to-gas ratio would be 1 10^{-3} (see Arndt et al. 1997, and our discussion of appropriate choices for the C:O ratio in Schröder et al. 1999).

6. Outlook and conclusions

The work presented here must be regarded as a first step towards deriving, from *first principles* of stellar astrophysics, the collective mass-loss and representative samples of the galactic stellar component. Despite the need of further improvement on several remaining simplifications, our synthetic stellar sample matches well the observed solar neighbourhood stellar sample (see Figs. 2 and 3), its mass-loss agrees well with the range of mass-loss rates derived from observations, and the absolute numbers of our tip-AGB stars can well accommodate the observed space-density of C-stars (Groenewegen 1992). Our synthetic stellar sample may, therefore, be seen as representative of the galactic disk stellar component in the mass-range of 1.0 to 2.5 $M_\odot$.

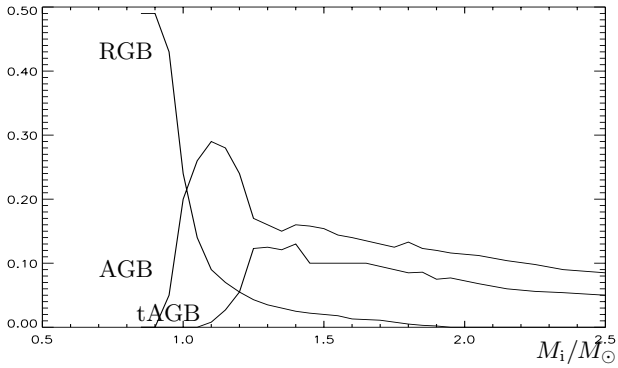

Fig. 9. The contributions (on an relative scale), of a sample of stars with γ(IMF)= -1.8, from any M_i-interval to the total collective stellar mass re-injection

Future theoretical improvements should aim at including upcoming consistent wind models for the oxygen-rich stars (Jeong et al. 1999), should account for non-solar metallicities (work in progress), and should consider binary stars.

More precise values for the dust-to-gas ratio of the stellar winds, and a self-consistent handling of the C:O abundance ratio on the stellar surface and in the wind, both depend on improvements in our evolution code towards a quantitative model of the mixing and third dredge-up process by thermal pulses.

Furthermore, we are working on presenting our synthetic sample in IR colours, which we will derive from interpolation and time-averaging of our wind models, as was already done by Le Bertre & Winters (1997). This will lead to a direct comparison with observed AGB star samples. In the future, this kind of analysis can be applied to the AGB giants of the galactic bulge observed by the ISOGAL project, and to the complete samples of Magellanic Cloud giants (Cioni et al. 2000), and it will provide a quantitative model of how cool wind mass-loss depends on metallicity.

With the above mentioned theoretical refinements in modelling the galactic stellar component, there is a bright future for synthetic stellar samples. Astrometric missions like FAME will provide much larger, complete stellar samples than *Hipparcos* did. These samples will include a large number of tip-AGB objects and their precise distances, and they will permit a more detailed study of IMF, SFR, and stellar diffusion between galactic bulge and halo. Interpreting these large, future data sets by means of synthetic stellar samples is a powerful tool, since only *complete* stellar samples reveal the *full* information. We therefore hope that this approach will lead to a new quality of input information for future, detailed galaxy models.

Conclusions:
We have derived the single star IMF and SFR of the solar neighbourhood in the most direct way: by distributing synthetic stars on evolution tracks to match, by star counts in crucial HR diagram regions, the observed (*Hipparcos*) local HR diagram.

Using the IMF and SFR of our best matching synthetic stellar sample based on our evolution models with a detailed, consistent mass-loss description, with a 1000-fold increase in the total number of stars, we have computed a representative, present-day sample of giants and tip-AGB stars, including their mass-loss rates. The relevant range of initial stellar masses is 1 to 2.5 $M_{\odot}$.

We have also been able to derive the collective yields of cool stellar winds, and the galactic disk mass re-injection from an important portion of the stellar component. This is a first step towards deriving relevant input parameters for galaxy models from *first principles*, i.e., from the available knowledge of stellar astrophysics rather than from approximative scaling laws.

Acknowledgements. This work has been supported by the DFG grants Se 420/12-1 to 12-3. Furthermore, we would like to thank the anonymous referee and Dr. L. J. Ball for their suggestions which greatly improved this publication.

References

Arndt, T. U., Fleischer, A. J., & Sedlmayr, E. 1997, A&A, 327, 614
Cioni, M.-R. L., van der Marel, R. P., Loup, C., & Habing, H. J. 2000, A&A, 359, 601
Dwek, E. 1998, ApJ, 501, 643
De Jager, C., Nieuwenhuijzen, H., & van der Hucht, K. A. 1988, A&AS, 72, 259
Eggleton, P. P. 1971, MNRAS, 151, 351
Eggleton, P. P. 1972, MNRAS, 156, 361
Eggleton, P. P. 1973, MNRAS, 163, 179
Fleischer, A. J., Gauger, A., & Sedlmayr, E. 1992, A&A, 266, 321
Glass, I. S., Ganesh, S., Alard, C., et al. 1999, MNRAS, 308, 127
Groenewegen, M. A. T., de Jong, T., van der Bliek, N. S., Slijkhuis, S., & Willems, F. J. 1992, A&A, 253, 150
Groenewegen, M. A. T., van den Hoek, L. B., & de Jong, T. 1995, A&A, 293, 381
Habing, H. J. 1994, A&AR, 7, 97
Herwig, F. 1996, Proc. 32nd Liège Intern. Astrophys. Coll. 1995, 441
Iben, Jr I., Tutukov, A. V., & Yungelson, L. R. 1996, ApJ, 456, 750
Jeong, K. S., Winters, J. M., & Sedlmar, E. 1999, Proc. IAU Symp. 191, ed. C. Waelkens, T. Le Bertre, & A. Lèbre, 233
Josselin, E., Blommaert, J. A. D. L., Groenewegen, M. A. T., Omont, A., & Li, F. L. 2000, A&A, 357, 225
Le Bertre, T., & Winters, J. M. 1998, A&A, 334, 173
Miller, G. E., & Scalo, J. M. 1979, ApJS, 41, 513
Olofsson, H., Bergman, P., Eriksson, K., & Gustafsson, B. 1996, A&A, 311, 587
Olofsson, H., Bergman, P., Lucas, R., et al. 2000, A&A, 353, 583
Omont, A., Ganesh, S., Alard, C., et al. 1999, A&A, 348, 755
Pols, O. R., Schröder, K.-P., Tout, C. A., Hurley, J. R., & Eggleton, P. P. 1998, MNRAS, 298, 525
Reimers, D. 1975, in Problems in Stellar Atmospheres and Envelopes ed. B. Baschek, & W. H Kegel (Springer, Berlin), 229
Renzini, A. 1981, in Physical Processes in Red Giants, ed. Jr. I. Iben, & A. Renzini (D. Reidel Publ. Co., Dordrecht, Holland), 431
Scalo, J. M. 1986, Fund. Cosm. Phys., 11, 1
Schröder, K.-P. 1998, A&A, 334, 901
Schröder, K.-P., Winters, J. M., Arndt, T. U., & Sedlmayr, E. 1998, A&A, 335, L9
Schröder, K.-P., Winters, J. M., & Sedlmayr, E. 1999, A&A, 349, 898
Sedlmayr, E. 1994, in IAU Colloquium 146 Molecules in the Stellar Environment, ed. U. G. Jørgensen (Springer–Verlag, Berlin), 163
Sedlmayr, E., & Winters, J. M. 1997, Stellar Atmospheres: Theory and Observations, vol. 497 of Lecture Notes in Physics, Chapter "Cool star winds and mass loss: Theory" (Springer, EADN Astrophysics School IX), 89
Wasserburg, G. J., Boothroyd, A. I., & Sackmann, I.-J. 1995, ApJ, 447, L37
Weidemann, V. 1997, Advances in Stellar Evolution (Cambridge University Press, UK), 169
Whitelock, P., Menzies, J., Feast, M., et al. 1994, MNRAS, 267, 711
Winters, J. M., Fleischer, A. J., Le Bertre, T., & Sedlmayr, E. 1997, A&A, 326, 305